Emission Spectra of LSO and LYSO Crystals Excited by UV Light, X-Ray and γ-ray

Rihua Mao, *Member, IEEE*, Liyuan Zhang, *Member, IEEE*, and Ren-Yuan Zhu, *Senior Member, IEEE*

Abstract—Because of their high stopping power ($X_0 = 1.14$ cm, $R_{\text{Moliere}} = 2.07$ cm) and fast (~ 40 ns) bright (4 times of BGO) scintillation, cerium doped lutetium oxyorthosilicate (LSO) and cerium doped lutetium-yttrium oxyorthosilicate (LYSO) crystals have attracted a broad interest in the high energy physics community. This paper presents a comparative study on emission spectra measured for large size BGO, lead tungstate (PbWO$_4$), LSO and LYSO samples excited by UV light (photo-luminescence) with and without internal absorption, x-ray (x-luminescence) and γ-ray (radio-luminescence). A red shift was observed between the emission spectra with internal absorption as compared to that without. An additional red shift and a significant red component were observed in the radio-luminescence spectra measured for LSO samples but not LYSO samples, which were disappeared after a γ-ray irradiation with an accumulated dose of 5×10^3 rad. This is the only significant difference observed between the large size LSO and LYSO samples. The origin of these red shifts and the consequence to their light output and applications in the high energy and nuclear physics experiments are discussed.

Index Terms—Crystal, lutetium oxyorthosilicate, lutetium yttrium oxyorthosilicate, photo-luminescence, radio-luminescence, scintillator, X-luminescence.

I. INTRODUCTION

BECAUSE of their high stopping power ($X_0 = 1.14$ cm, $R_{\text{Moliere}} = 2.07$ cm) and fast (~ 40 ns) bright (4 times of BGO) scintillation, cerium doped lutetium oxyorthosilicate (Lu$_2$SiO$_5$:Ce, LSO) and cerium doped lutetium-yttrium oxyorthosilicate (Lu$_{2(1-x)}$Y$_{2x}$SiO$_5$:Ce, LYSO) crystals have attracted a broad interest in the high energy physics community for future experiments, such as a super B factory [1] and the international linear collider (ILC) [2].

Starting 2005 a DOE supported advanced detector R&D program has been carried out at Caltech to investigate the optical and scintillation properties of large size ($2.5 \times 2.5 \times 20$ cm) LSO and LYSO crystal samples [3]–[5]. While the overall properties of LSO and LYSO samples were found to be consistent, about 15% more light output was observed for our first large size LSO sample CTI-LSO-L1 from CTI Molecular Imaging (CTI) by using a Hamamatsu S8664-55 avalanche photodiode (APD) based readout as compared to LYSO samples of the same size [6]. This observation is in contrast with
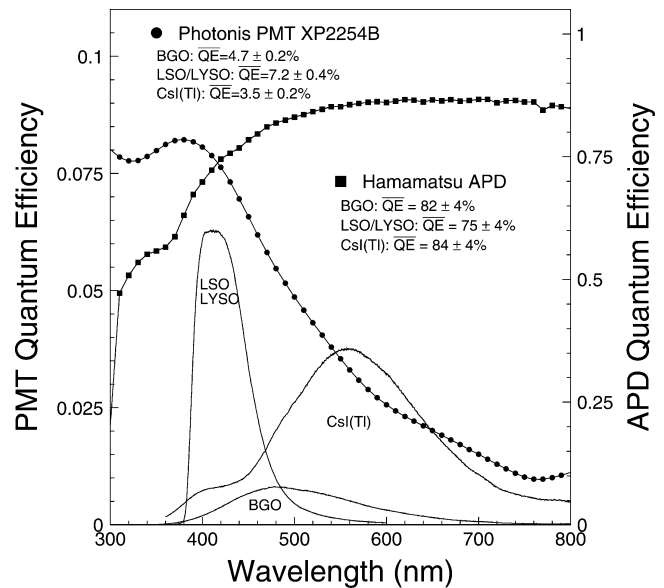

Fig. 1. Quantum efficiencies of a Photonis XP2254B PMT (solid dots) and a Hamamatsu S8664 APD (solid squares) are shown as a function of wavelength together with the UV excited emission spectra of the LSO/LYSO, BGO and CsI(Tl) samples, where the area under the emission curves is roughly proportional to corresponding absolute light output.

what observed by using a Photonis XP2254B photomultiplier (PMT) based readout, where no such difference was observed. This discrepancy between the APD and PMT data was reported in the 2005 Nuclear Science Symposium at Puerto Rico as shown respectively in Figs. 10 and 6 of [6]. Furthermore, this discrepancy was found disappeared after the CTI-LSO-L1 sample went through an irradiation with an accumulated ^{60}Co dose of 1 Mrad followed by a thermal annealing at 300°C for ten hours [5].

Fig. 1 shows the quantum efficiencies of the PMT and APD used in these measurements. Also shown in this figure is the LSO/LYSO's photo-luminescence spectrum without internal absorption. A larger light output with the APD readout may be explained by a long wavelength component in the LSO emission as compared to the LYSO emission, which disappeared after the ^{60}Co irradiation and the thermal annealing.

In this paper, we present a study on various emission spectra for large size BGO, lead tungstate (PbWO$_4$, PbWO$_4$), LSO and LYSO samples excited by UV light (photo-luminescence), x-ray (x-luminescence) and γ-ray (radio-luminescence). The result of this study shows indeed that a long wavelength component exists in the radio-luminescence spectra of the LSO samples, but not the LYSO samples. In addition, this long wavelength component is not affected by thermal annealing, but disappears after

Fig. 2. Photo showing six LSO/LYSO crystal samples used in this study.

γ-ray irradiations. These observations explain well the discrepancy reported in Puerto Rico conference. The nature of this long wavelength component in LSO and its consequence to the application in high energy physics are also discussed.

II. SAMPLES

Fig. 2 shows six samples used in this study. They are, from top to bottom, three CTI LSO samples (CTI-LSO-L1, CTI-LSO-L2 and CTI-LSO-L3) provided by Dr. Chuck Melcher and three LYSO samples procured from Saint-Gobain Ceramics & Plastics, Inc. (SG-LYSO-L1, SG-LYSO-L2 and SG-LYSO-L3). All samples are long rectangular bar with a dimension of $2.5 \times 2.5 \times 20$ cm^3. According to the manufacturers, the nominal cerium doping level is 0.2% for the CTI LSO samples and less than 1% for the Saint-Gobain LYSO samples. The yttrium fraction in LYSO samples is about 10%.

III. EXPERIMENTAL APPARATUS

Fig. 3 shows a setup used for the emission measurement. The photo-luminescence spectra were measured by using a Hitachi F-4500 fluorescence spectrophotometer with the excitation wavelength fixed, so that the intensity of the emission light is maximized. This is 304 nm, 310 nm and 358 nm for BGO, PbWO$_4$ and LSO/LYSO respectively. The UV excitation light was shot to a bare surface of the crystal sample, and the sample was oriented with an angle θ between its surface normal and the excitation light. In the case of $\theta = 10°$, the measured photo-luminescence light is not affected by sample's internal absorption. In the case of $\theta = 0°$, the measured emission light goes through the sample body, so is affected by the internal absorption. For both x-luminescence and radio-luminescence measurements the sample was wrapped by two layers of Tyvek paper. For the x-luminescence measurement the sample was placed in F-4500's sample compartment with a small hole made on the Tyvek paper to allow x-ray generated by an Amptek E3-T X-ray tube passing, as shown in Fig. 3. The

x-luminescence spectra were measured by using F4500. For the radio-luminescence measurement a large fraction of sample's body was exposed to a ^{60}Co source. The radio-luminescence spectra were measured by a home made spectrophotometer. The emission light from the sample was first modulated by an optical chopper and then passed through a monochromator. A Photonis XP2254B with a multi-alkali cathode was used to detect the photons at the monochromator exit with the signal read out by a lock-in amplifier (Oriel Merlin system). The emission light excited by both X-ray and γ-ray is affected by the internal absorption.

Emission spectra of a BGO sample and a PbWO$_4$ sample were measured. Both samples are provided by Shanghai Institute of Ceramics (SIC), and have similar dimensions as the LSO and LYSO samples. Figs. 4 and 5 show the emission spectra of the BGO and PbWO$_4$ samples respectively. While the photo-luminescence measured with internal absorption ($\theta = 0°$, black), x-luminescence (green) and radio-luminescence (red) spectra are consistent, a red shift was observed between these spectra and the photo-luminescence without internal absorption ($\theta = 10°$, blue). This red shift is about 15 nm and 20 nm for BGO and PbWO$_4$ samples respectively, which can be explained by the internal absorption. We note that weighting a photo-luminescence spectrum without internal absorption with sample's longitudinal transmittance data would lead to a spectrum consistent with the luminescence spectra with internal absorption. The PbWO$_4$ sample shows a larger red shift than the BGO sample since its emission is closer to the absorption edge as discussed in [7]. The consistency of the photo-luminescence measured with internal absorption ($\theta = 0°$), the x-luminescence and the radio-luminescence, which was measured by an entirely independent system, indicates that the optics of both systems are well calibrated for these measurements.

IV. LYSO AND LSO EMISSION

Fig. 6 shows the emission spectra of SG-LYSO-L1. All other LYSO samples show the same spectra. A much larger red shift is observed between the luminescence spectra with and without internal absorption, indicating a strong self-absorption effect as discussed in [7] and [3]. While the photo-luminescence with internal absorption ($\theta = 0°$) and the radio-luminescence are more or less consistent, it is interesting to note that the x-luminescence is slightly narrower. This is observed for all LSO and LYSO samples. Since there is no difference in either the light path or the sample wrapping for the x-luminescence and the radio-luminescence measurements the only difference seems the excitation source. The penetration depths of these excitation sources are summarized in Table I. One notes that among these three excitation sources the X-ray has the shortest penetration depth of about 10 μm. The narrow x-luminescence is thus suspected to be caused by a surface effect, where the distorted crystal lattice structure affects the luminescence centers.

Figs. 7 and 8 show the emission spectra of CTI-LSO-L1 and CTI-LSO-L3 respectively. While the sample CTI-LSO-L3 is as-received, the sample CTI-LSO-L1 was used in our 2005 measurement [6] and went through a ^{60}Co γ-ray irradiation of 1 Mrad and a thermal annealing at 300°C for ten hours [5]. While the emission spectra of CTI-LSO-L1 are more or less
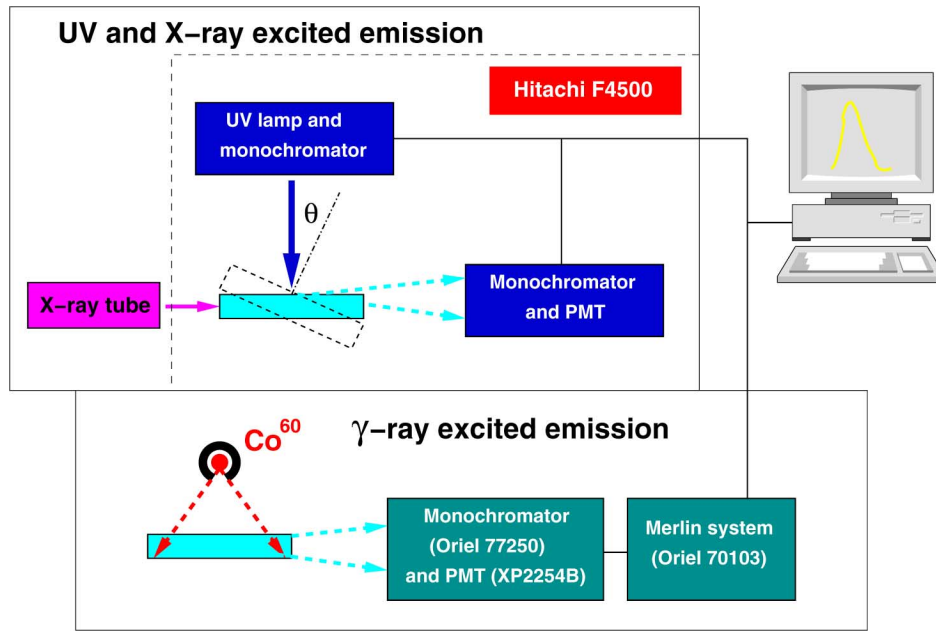
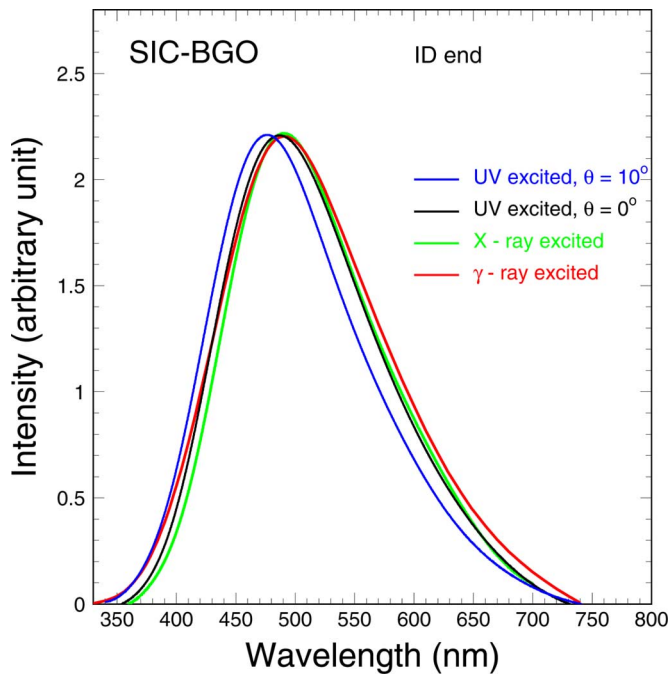Fig. 3. Setup used for the measurements of the emission spectra excited by UV light, X-ray and γ-ray.

Fig. 4. Emission spectra of a SIC BGO sample excited by UV light, X-ray and γ-ray are shown as a function of wavelength.
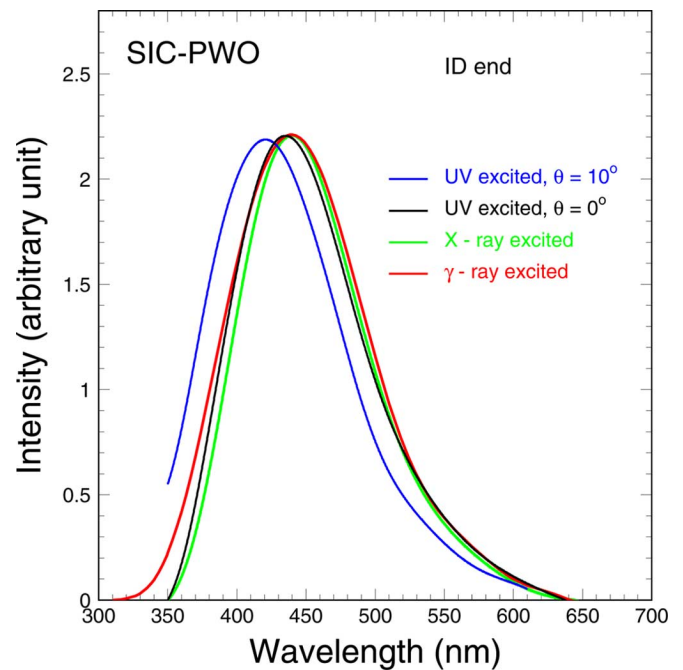

Fig. 5. Emission spectra of a SIC PbWO$_4$ sample excited by UV light, X-ray and γ-ray are shown as a function of wavelength.

similar to that of SG-LYSO-L1, the radio-luminescence spectrum of CTI-LSO-L3 is broader, indicating a long wavelength component, and has another red shift of about 20 nm. This broad and red-shifted radio-luminescence spectrum explains why the as-received CTI-LSO-L1 sample shows 15% more light output with the APD readout but not with the PMT readout.

Similar emission spectra were observed for the as-received samples CTI-LSO-L2 and CTI-LSO-L3. Our initial suspicion was that the thermal annealing at 300°C for ten hours applied to CTI-LSO-L1 changed its radio-luminescence spectrum. To

verify that a systematic thermal annealing test was carried out for the samples CTI-LSO-L2 and SG-LYSO-L2 from 300°C to 600°C with an 100°C increment and ten hours in each step. Fig. 9 shows the radio-luminescence spectra measured for as-received CTI-LSO-L2 (red), after the 400°C thermal annealing (green) and after the 600°C thermal annealing (blue). No variation was observed in the radio-luminescence spectra during the entire test for both LSO and LYSO samples.

Finally, both CTI-LSO-L2 and SG-LYSO-L2 went through a ^{60}Co γ-ray irradiation with an accumulated dose of about
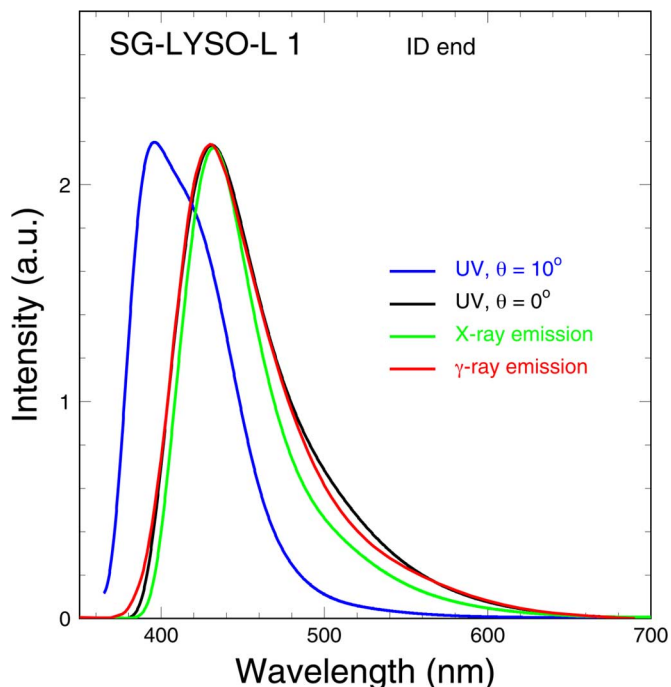
Fig. 6. Emission spectra of SG-LYSO-L1 excited by UV light, X-ray and γ-ray are shown as a function of wavelength.
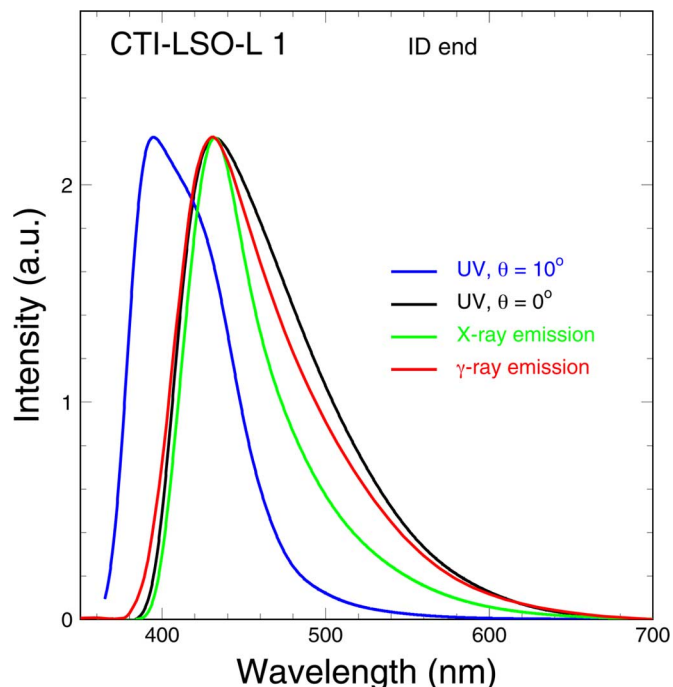

Fig. 7. Emission spectra of the sample CTI-LSO-L1 after a γ-ray irradiation and a thermal annealing, excited by UV light, X-ray, and γ-ray are shown as a function of wavelength.

TABLE I
DEPTHS OF EXCITATION SOURCES IN LSO/LYSO CRYSTALS

Excitation Source	Penetration depth
UV light	$100 \sim 700 \ \mu m$
X-ray (8-30 keV)	$\sim 10 \ \mu m$
γ-ray ($Co^{60}, \sim 1.2$ MeV)	$\sim 1.14 \ cm$

5×10^3 rad. The radio-luminescence spectrum measured for CTI-LSO-L2 after the irradiation was blue-shifted by 20 nm with result similar to what observed in Fig. 7. The sample SG-LYSO-L2, however, shows no change in the emission spectra. It thus is clear that γ-ray irradiations changed the radio-luminescence only for the LSO samples.

V. EMISSIONS OF HALF IRRADIATED SAMPLES

To verify that the γ-ray irradiation indeed changes the radio-luminescence of LSO not LYSO a lead shielding fixture was constructed to shield a half sample during irradiations with ^{60}Co γ-rays. Two samples, CTI-LSO-L3 and SG-LYSO-L3, were irradiated this way with an accumulated dose of about 5×10^3 rad. Figs. 10 and 11 compare the radio-luminescence spectra of the irradiated half (ID end) and the non-irradiated half (NID end) for CTI-LSO-L3 and SG-LYSO-L3 respectively after the irradiation. It is clear that the irradiated half (ID end) of CTI-LSO-L3 shows a narrower and blue-shifted radio-luminescence as compared to the non-irradiated half (NID end), while no change in radio-luminescence was observed in the SG-LYSO-L3 sample. This result confirmed our observations obtained from the samples CTI-LSO-L2 and SG-LYSO-L2.

Figs. 12 and 13 show the light output and the decay kinetics of two halves of CTI-LSO-L3 measured before and after the γ
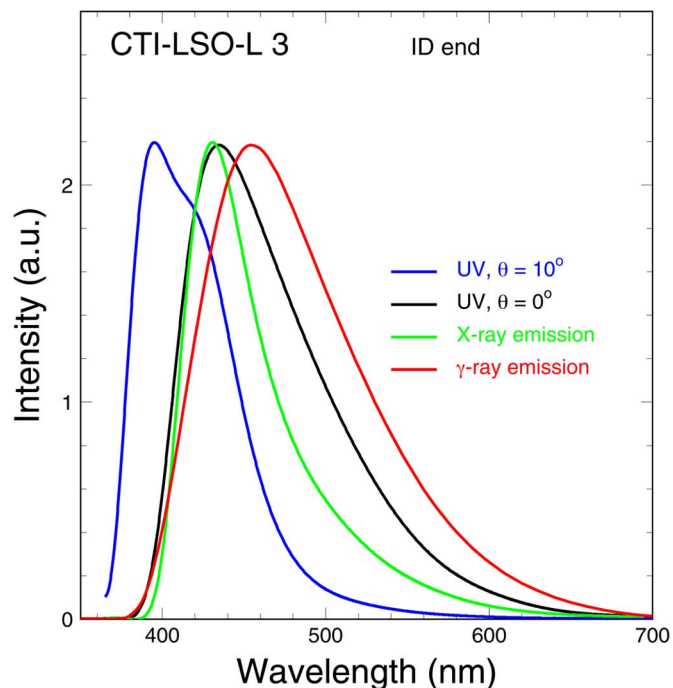

Fig. 8. Emission spectra of the as-received CTI-LSO-L3 excited by UV light, X-ray, and γ-ray are shown as a function of wavelength.

irradiation to the ID-end half. While no change was found in the decay kinetics between two halves of the sample, the relative light output degradation of the irradiated half is only about half of that of the non irradiated half. Since the signal light went through similar light path in both measurements this difference is consistent with the blue shift of the radio-luminescence of the irradiated half because of the high quantum efficiency of
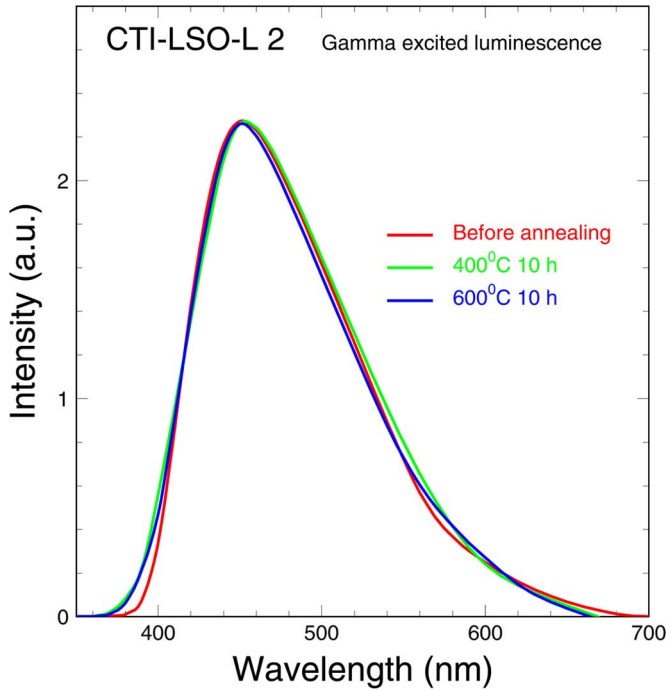
Fig. 9. Radio-luminescence spectra of CTI-LSO-L2 measured before and after thermal annealing at 400°C and 600°C.
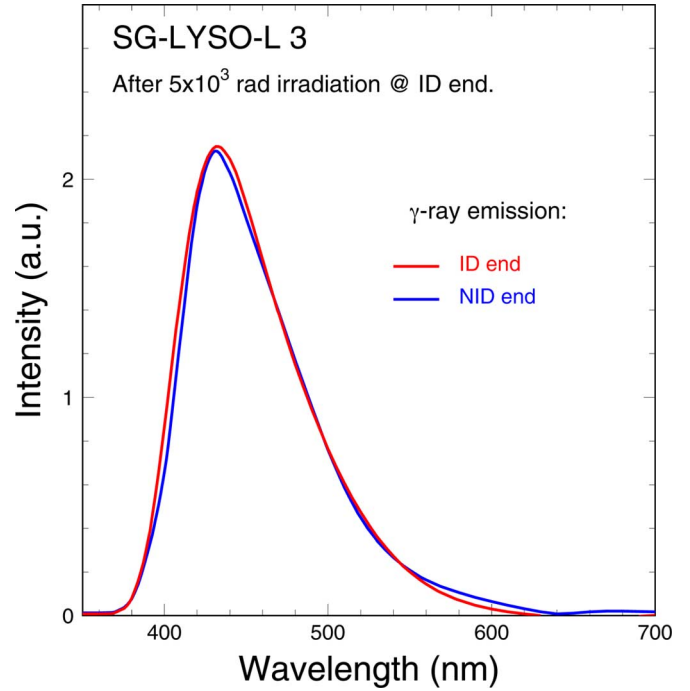

Fig. 11. γ-ray excited emission spectra of the two halves of SG-LYSO-L3. ID end is the half that received a γ dose of 5×10^3 rad, and NID end is the half did not.
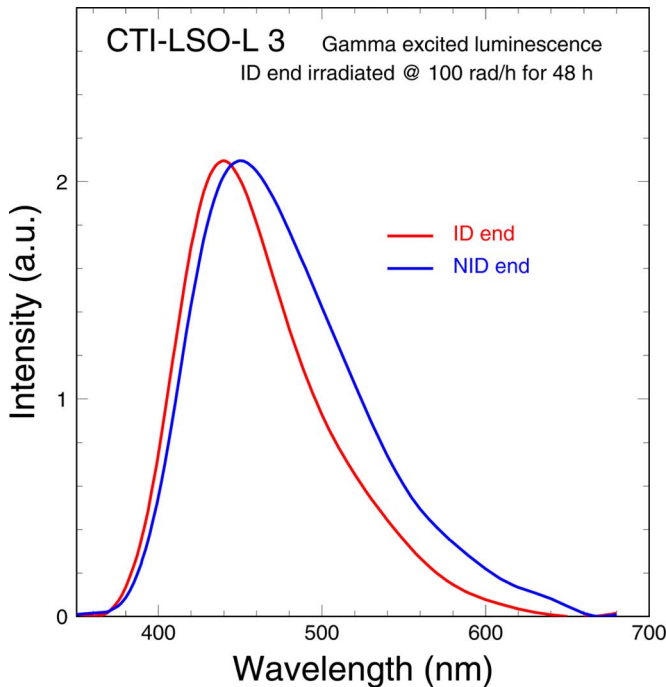

Fig. 10. γ-ray excited emission spectra of the two halves of CTI-LSO-L3. ID end is the half that received a γ dose of 5×10^3 rad, and NID end is the half did not.

Fig. 12. Light output and decay kinetics, measured using the XP2254B PMT for the ID-end half of CTI-LSO-L3 before and after a γ dose of 5×10^3 rad, are shown as a function of the integration time.

VI. DISCUSSION ABOUT THE LSO RED EMISSION

As shown in Table I the penetration depth of the UV excitation light is sub-millimeter. The long wavelength component observed in the radio-luminescence spectrum should also be observed in the photo-luminescence spectra by using different excitation wavelength. A scan was carried out to measure the photo-luminescence spectra as a function of the wavelength of the UV-excitation light by using the Hitachi F4500 spectrophotometer to reveal the interplay between the excitation

the XP2254B PMT at the short wavelength. No such variations were found between two halves of the SG-LYSO-L3 sample. In addition, results of the light response uniformity measurements are also consistent with this conclusion.
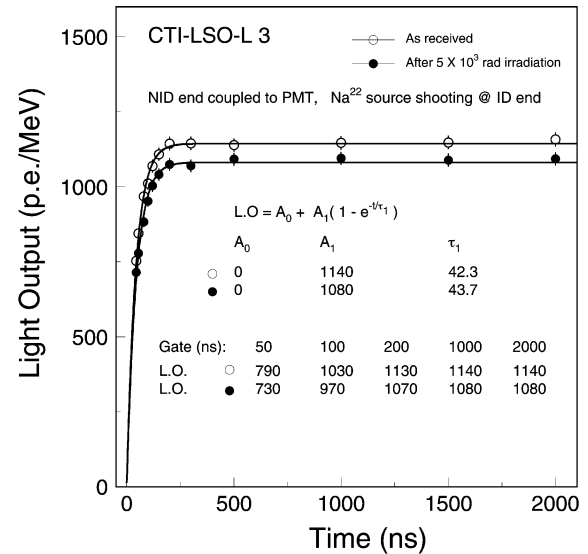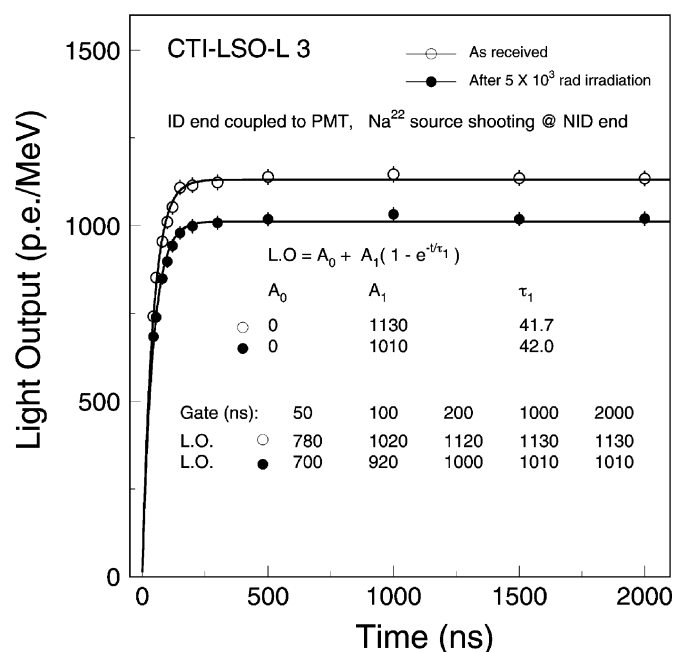
Fig. 13. Light output and decay kinetics, measured using the XP2254B PMT for the NID-end half of CTI-LSO-L3 before and after a γ dose of 5×10^3 rad, are shown as a function of the integration time.
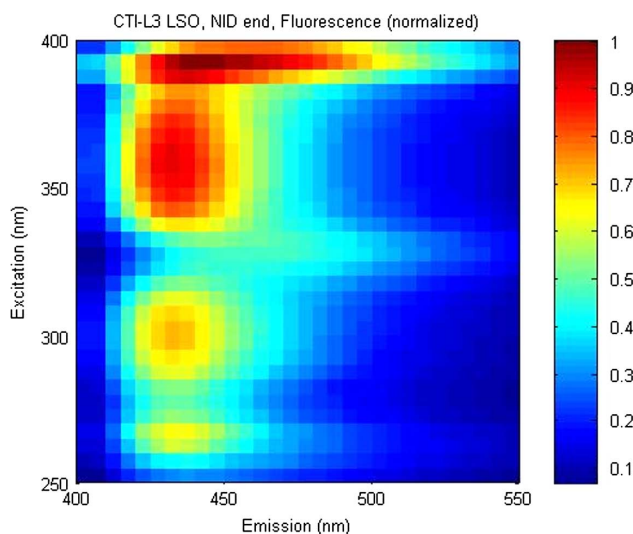

Fig. 14. Two dimensional distribution of the UV-excitation and the photo-luminescence spectra for the non-irradiated half of CTI-LSO-L3.
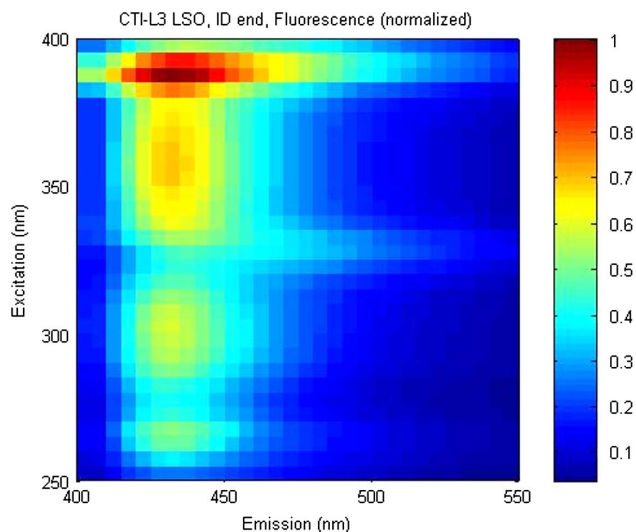

Fig. 15. Two dimensional distribution of the UV-excitation and the photo-luminescence spectra for the irradiated half of CTI-LSO-L3.
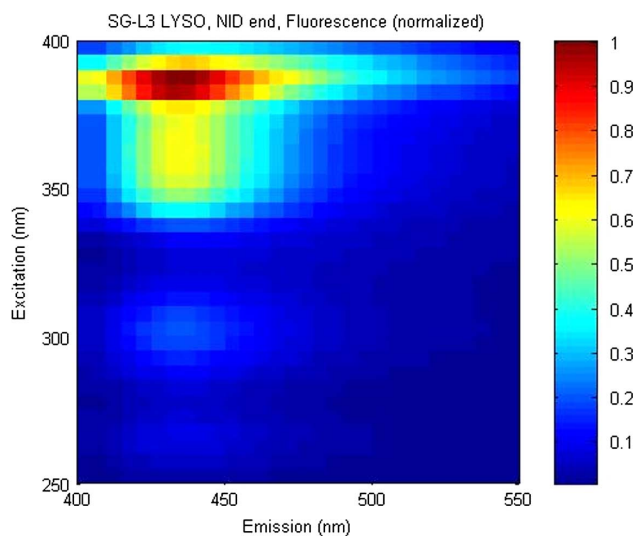

Fig. 16. Two dimensional distribution of the UV-excitation and the photo-luminescence spectra for the non-irradiated half of SG-LYSO-L3.

and emission spectra. Figs. 14, 15, 16 and 17 show two-dimension distributions of the UV-excitation and photo-luminescence spectra for two halves of CTI-LSO-L3 and SG-LYSO-L3 respectively with the maximum of the emission intensity normalized to one. As shown in Fig. 14, the non-irradiated half of CTI-LSO-L3 contains long wavelength components with the excitations wavelength at 325 nm and 380 nm. These red components are significantly reduced in the irradiated half of CTI-LSO-L3, as shown in Fig. 15. No such long wavelength components were observed in the SG-LYSO-L3 sample, as shown in Figs. 16 and 17. This result is consistent with what observed in the radio-luminescence spectra.

The emission mechanism and the Ce^{3+} luminescence centers in LSO have been investigated at low temperature [8], [9]. In [9], J. D. Naud *et al.* concluded that there are two kinds of Ce^{3+} luminescence centers in LSO. The dominating one, Ce1, is the crystallographic sites of Lu atoms, and the minor one Ce2 is a kind of irregular site. They proposed that Ce2 is some interstitial sites because no typical doublet emission structure was observed even at 13°K. According to this model, the long wavelength emission component is caused by Ce2. The fact that the emission spectra of Ce2 can be modified by the γ-ray irradiation, however, supports an assumption that it probably is a defect perturbed regular sites of Ce^{3+}. During the γ-ray irradiation, the defects may capture a charge (electron or hole) and its perturbation to the energy levels of Ce^{3+} may be significantly decreased. Figs. 18 and 19 show a close look of these two sites for both halves of CTI-LSO-L3 and SG-LYSO-L3 respectively. The emission spectrum of the Ce2 site excited at 325 nm (bottom plot) was changed by the γ-ray irradiation for
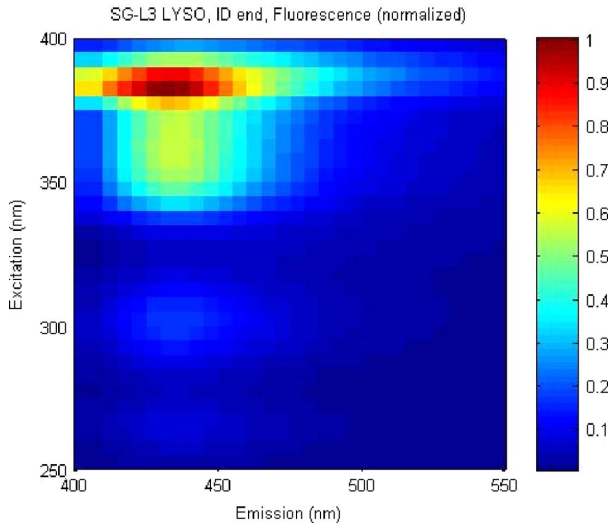
Fig. 17. Two dimensional distribution of the UV-excitation and the photo-luminescence spectra for the irradiated half of SG-LYSO-L3.
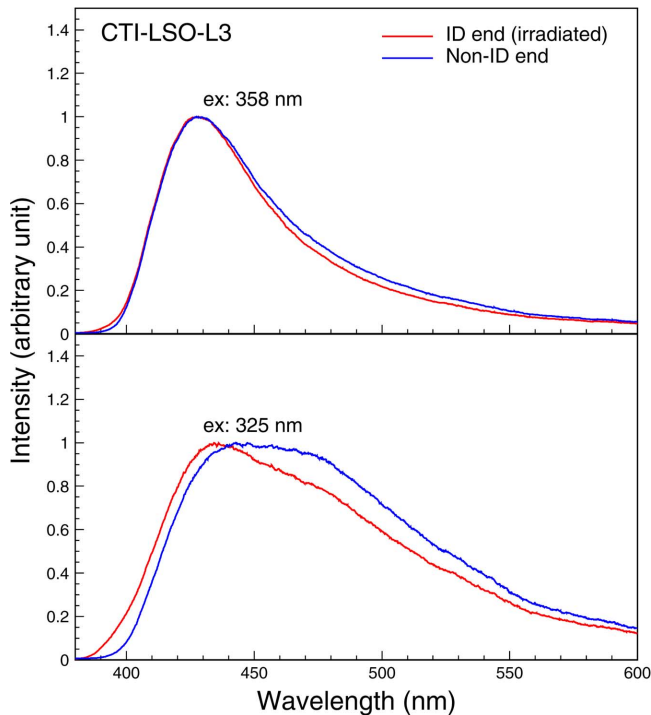

Fig. 18. Comparison of the photo-luminescence spectra for CTI-LSO-L3. Top: Ce1 site excited at 358 nm and bottom: Ce2 site excited at 325 nm. The ID end is the irradiated half and the non-ID end is the non-irradiated half.
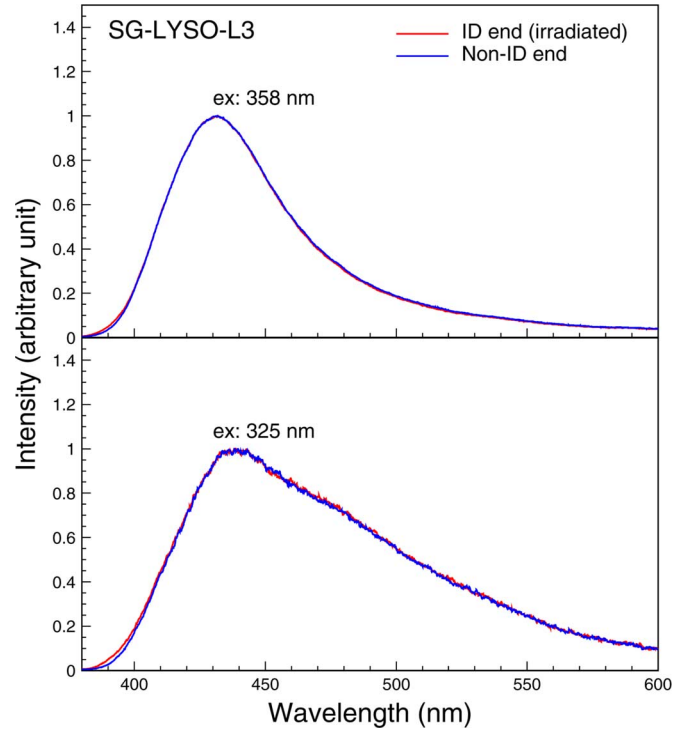

Fig. 19. Comparison of the photo-luminescence spectra for SG-LYSO-L3. Top: Ce1 site excited at 358 nm and bottom: Ce2 site excited at 325 nm. The ID end is the irradiated half and the non-ID end is the non-irradiated half.

CTI-LSO-L3, while the emission spectra of the Ce1 site excited at 358 nm was not changed. Both the emissions excited at 358 nm and 325 nm are not changed by γ-ray irradiations for the SG-LYSO-L3 sample. Judging from the data, the density of Ce2 centers seems very low in LYSO, or was greatly reduced by the yttrium doping.

VII. SUMMARY

A red-shift was observed between the photo-luminescence measured with $\theta = 0°$, the x-luminescence and the radio-luminescence versus the photo-luminescence measured with $\theta = 10°$ in all crystal scintillators, which is caused by the internal absorption. This red-shift is much stronger for LSO/LYSO samples since part of its emission is self-absorbed. The x-luminescence spectra of the LSO/LYSO samples are narrow as compared to other emission spectra, which seems caused by a surface effect.

A broader radio-luminescence spectrum with an additional red-shift was observed in as-grown LSO samples as compared to the photo-luminescence measured with $\theta = 0°$ and x-luminescence spectra. This additional red-shift disappeared after γ-ray irradiations with an accumulated dose of as low as 5×10^3 rad, but was not affected by thermal annealing. This observation consists with the light output and uniformity data, and can explain the high light output observed with APD readout reported in [6].

We tentatively attribute this red-shift to the contribution of the irregular luminescence center Ce2. The fact that it can be cured more or less by γ-ray irradiations supports that this site is a defect perturbed irregular site of Ce^{3+}. No such shift was observed in LYSO samples. The yttrium doping seems reduces the density of, or eliminates, the defect perturbed irregular site of Ce^{3+}. This is the only difference observed between LSO and LYSO samples.

REFERENCES

[1] W. Wisniewski, R.-Y. Zhu, Ed., "Consideration for calorimetry at a super B factory," in *Proc. 10th Int. Conf. Calorimetry in Particle Physics*, Mar. 2002.

[2] R.-Y. Zhu, "An LSO/LYSO crystal calorimeter for the ILC," presented at the Int. Linear Collider Physics Detector Workshop and 2nd ILC Accelerator Workshop, Snowmass, CO, Aug. 14–27, 2005.

[3] J. M. Chen, L. Y. Zhang, and R. Y. Zhu, "Large size LYSO crystals for future high energy physics experiments," *IEEE Trans. Nucl. Sci.*, vol. 52, no. 6, pp. 3133–3142, Dec. 2005.

[4] J. M. Chen, R. H. Mao, L. Y. Zhang, and R. Y. Zhu, "Large size LSO and LYSO crystal for future high energy and nuclear physics experiments," *IEEE Trans. Nucl. Sci.*, vol. 54, no. 3, pp. 718–724, Jun. 2007.

[5] J. M. Chen, R. H. Mao, L. Y. Zhang, and R. Y. Zhu, "Gamma-ray induced radiation damage in large size LSO and LYSO crystal samples," *IEEE Tran. Nucl. Sci.*, vol. 54, no. 4, pp. 1319–1326, Aug. 2007.

[6] J. M. Chen, L. Y. Zhang, and R. Y. Zhu, "A further study on large size LSO and LYSO crystals samples," presented at the NSS Conference Rec., 2005, Paper N12-6,.

[7] R. H. Mao, L. Y. Zhang, and R. Y. Zhu, "Optical and scintillation properties of inorganic scintillators in high energy physics," *NSS 2007 Conf. Rec.*, vol. N49-1, 2007.

[8] H. Suzuki, T. A. Tombrello, C. L. Melcher, and J. S. Schweitzer, "Light emission mechanism of $Lu_2(SiO_4)O$: Ce," *IEEE Tran. Nucl. Sci.*, vol. 40, no. 4, pp. 380–383, Aug. 1993.

[9] J. D. Naud, T. A. Tombrello, C. L. Melcher, and J. S. Schweitzer, "The role of Cerium sites in the scintillation mechanism of LSO," *IEEE Tran. Nucl. Sci.*, vol. 43, no. 3, pp. 1324–1328, Jun. 1996.